Fall 2020

A Cloning Strategy for Expression of Fungal Hemicellulases in Plant Systems

Amer Alrudayan
Eastern Illinois University

A Cloning Strategy for Expression of Fungal Hemicellulases in Plant Systems

by

Amer Alrudayan

THESIS

SUBMITTED IN PARTIAL FULFILLMENT OF THE REQUIREMENTS

FOR THE DEGREE OF

MASTER OF SCIENCE

IN BIOLOGICAL SCIENCES

IN THE GRADUATE SCHOOL, EASTERN ILLINOIS UNIVERSITY

CHARLESTON, ILLINOIS

2020

I HEREBY RECOMMEND THAT THIS THESIS BE ACCEPTED AS FULFILLING THIS PART OF THE GRADUATE DEGREE CITED ABOVE

THESIS COMMITTEE CHAIR	DATE	DEPARTMENT CHAIR	DATE
THESIS COMMITTEE MEMBER	DATE	THESIS COMMITTEE MEMBER	DATE
THESIS COMMITTEE MEMBER	DATE	THESIS COMMITTEE MEMBER	DATE

Abstract

Lignocellulosic biomass is notoriously difficult to deconstruct into lignin, hemicellulose, and cellulose fractions without the use of biochemical, chemical, and/or mechanical pretreatments. These pretreatment strategies add operational cost and in some cases produce hazardous waste that poses health and safety risks. Direct biological pretreatment from biomass-degrading bacteria and fungi may significantly reduce the costs and risks associated with these traditional strategies due to the innate ability of these organisms to modify plant cell walls. An additional measure that could further reduce the expenses associated with lignocellulosic biomass fractionation is genetic modification of the lignocellulosic feedstocks, which can be accomplished by misregulating native genes and/or expressing foreign genes. In the present study, the genes for two hemicellulose-modifying enzymes, acetyl xylan esterase (AXE) and endo-polygalacturonase (EPG), were cloned from a white-rot fungus, *Trametes versicolor*, for the purposes of expressing these genes in plant systems. It was hypothesized that expression of these fungal enzymes in plants will reduce the covalent linkages in lignocellulose, particularly among the hemicellulose components of the cell wall. The AXE and EPG genes were subcloned into an entry plasmid, pDONR221, using Gateway technology, and were then transferred to binary plasmids (pEarleyGate backbones) suitable for *Agrobacterium*-mediated plant transformation. The genes are under the control of the 35S promoter with and without fluorescent protein fusions (CFP, YFP, or GFP). Future experiments will investigate the effects of these fungal hemicellulases on plant cell wall chemistry and digestibility in a variety of host systems (e.g. arabidopsis, tobacco, hybrid poplar), and explore the subcellular location of the enzymes using fluorescent microscopy.

Table of Contents

List of Tables and Figures

1. Introduction

Fossil fuels are well known to cause harm to natural environments and negatively impact ecosystems. Spillage of oil in marine environments because of shipping transport has caused pollution and impacted organisms that live in these environments (Troisi et al., 2016). Moreover, fossil fuels have a relationship with increasing CO_2 in the atmosphere, which contributes to the greenhouse effect (Shafiei and Salim, 2014). Thus, dependence on fossil fuels, and it is production, negatively affects the environment and human civilization. As stated by Lin et al. (2016), the global warming problems related to greenhouse gas pollution is greatly affected by the fossil fuel industry. According to McKendry (2002), to achieve changes required to resolve the problems of climate change, the usage of renewable energy sources is increasingly needed. Replacing or reducing fossil fuel use would also provide significant cultural and social advantages (Ciriminna, 2019).

Among the alternative and renewable energy sources available is bioenergy, which broadly encompasses energy derived from animal waste and plant matter. Under the bioenergy umbrella are liquid fuels (e.g. ethanol) that are derived from the starch and non-starch parts of plants. Starch-based biofuel production provides nearly all of the biologically-derived ethanol in the U.S., with insignificant commercial production of non-starch (lignocellulosic) ethanol (Renewable Fuels Association, 2017). The recalcitrance to deconstruction is the primary obstacle for biofuel production from non-starch biomass, such as wood and crop residue (Zhao et al., 2012).

The resistance to decomposition by plant cell walls is attributed to the covalent interconnectivity of the major polymers (cellulose, hemicellulose, and lignin) involved in

their construction, which collectively comprises lignocellulose. To access the individual components of this material (e.g. glucose from cellulose), pretreatment of biomass is required to deconstruct lignocellulose for biofuel applications, such as ethanol fermentation (Sanchez, 2009). For instance, physical pretreatment includes the degradation of crystallinity and biomass thickness. Typically, a large amount of energy is necessary for this process, which reduces its industrial utility. Chemical pretreatments, such as alkaline pretreatment, may also be necessary to prepare lignocellulose for downstream processes (Sanchez and Cardona, 2008); however, these treatments require specialized equipment and handling of hazardous materials and waste. As a result, biological pretreatments have been identified as potential alternatives that may reduce cost as well as environmental effects (Kumar et al., 2009).

Some of the most effective and well-studied biological pretreatment agents are white-rot fungi, whose inherent capacity to degrade lignocellulose through biochemical pathways has evolved for hundreds of millions of years (Floudas et al., 2012). Apart from wood-rich substrates, these fungi can deconstruct a variety of commercially produced lignocellulosic substrates, including rice and wheat bran, canola straw, miscanthus, and sunflower stems (Canam et al., 2011; Okamoto et al., 2011; Alaradi, 2017; Kalinoski et al., 2017; Alanazi, 2018; Alsubaie, 2019). These organisms are specialists at breaking down and altering the lignin portion of lignocellulose using enzymes and chemical compounds, including reactive oxygen species, at moderate temperatures (Canam et al., 2013a).

A significant amount of research has been devoted to examining the effects of white-rot fungi on lignocellulose by growing them directly on the substrate of interest

(Canam et al., 2011; MacDonald et al., 2011; MacDonald and Master, 2012; Suzuki et al., 2012; Kalinoski et al., 2017), which has the potential to enhance the efficiency of biofuel processes by reducing the severity of subsequent biomass processing (Canam et al., 2013a and 2013b). However, an additional strategy to mitigate some of the expenses associated with deconstructing biomass for bioenergy purposes is through genetic modification of plants. For example, field-grown transgenic hybrid poplar with down-regulated cinnamoyl-CoA reductase (CCR) showed improved glucose liberation and ethanol yields (Van Acker et al., 2014). In addition to modifying expression of native enzymes in plant species, studies have also investigated *in planta* expression of foreign lignocellulose-modifying enzymes from microbes, such as *Phanerochaete carnosa* (Tsai et al., 2012; Gandla et al., 2015) and *Hypocrea jecorina* (Wang et al., 2020). However, these studies are limited and warrant further investigation, especially with enzymes from white-rot fungi, which have a formidable suite of enzymes uniquely specialized for plant cell wall deconstruction.

Although many of the lignocellulose-modifying enzymes from white-rot fungi have the potential to influence cell wall structure when expressed directly in plant systems, those that degrade or otherwise compromise cellulose have the potential to be counterproductive for industrial applications that require high glucose yields (e.g. ethanol fermentation). Enzymes that act on lignin, especially those that require redox reactions or radical formation, may be undesirable due to the non-specific and unpredictable nature of their activity. In contrast, hemicellulases may be ideally suited for *in planta* expression in plants destined for biofuel processes. They typically have very specific activity and are unlikely to significantly compromise glucose yield. Instead, this category of enzymes is

capable of reducing the number and/or types of covalent linkages in lignocellulose, which may render the cell walls less recalcitrant to downstream processing.

2. Objectives

1. Identify hemicellulose-modifying enzymes from the core set of transcripts of *Trametes versicolor*, a white-rot fungus, grown on maple, miscanthus, and sunflower.
2. Clone genes of interest from *T. versicolor* cDNA into an entry plasmid using Gateway technology.
3. Use Gateway technology to transfer the genes of interest from entry plasmids to specialized destination plasmids.
4. Transform *Agrobacterium tumefaciens* with destination plasmids for future plant transformation and phenotype analysis.

3. Methods

3.1. cDNA Synthesis

Total RNA samples from a previous experiment with *Trametes versicolor* (52J; ATCC#: 20869) grown on sunflower stems for six weeks (Alsubaie, 2019) were used to generate cDNA. Residual DNA was removed from the RNA using the TURBO DNA-*free*™ Kit (Invitrogen; cat#: AM1907) according to the manufacturer's instructions. The DNase-treated RNA was then used to generate cDNA with the SuperScript™ III First-Strand Synthesis System for RT-PCR (Invitrogen; cat# 18080051). Briefly, 1 µg of RNA (adjusted to total volume of 8 µL with DEPC-treated water) was added to 1 µL of 50 µM

oligo(dT)$_{20}$ primer and 1 µL of 10 mM dNTP mix. This mixture was incubated at 65°C for 5 min and then placed on ice. This solution was then mixed with 2 µL of 10X RT buffer, 4 µL of 25 mM $MgCl_2$, 2 µL of 0.1 M DTT, 1 µL of RNaseOUT (40 U/µL), and 1 µL of SuperScript III (200 U/µL). The 20 µL mixture was then incubated at 50°C for 50 min, followed by 85°C for 5 min to stop the reaction. The cDNA was then treated with 1 µL of RNase H followed by incubation for 20 min at 37°C to remove residual RNA. Aliquots (3 µL) of each of the *T. versicolor*/sunflower cDNA samples were pooled prior to PCR amplification of the genes of interest.

3.2. Primer and Plasmid Design

The coding sequence of acetyl xylan esterase (AXE; transcript ID: 44147) and endo-polygalacturonase (EPG; transcript ID: 52686) were acquired from the *T. versicolor* transcript file (Trave1_GeneCatalog_transcripts_20101111.nt) available from the JGI Genome Portal (Floudas et al., 2012). For Gateway cloning (BP reaction) into pDONR^{TM}221 the forward and reverse primers are shown in Table 1.

Table 1. Primers used for amplifying acetyl xylan esterase (AXE) and endo-polygalacturonase (EPG) from *Trametes versicolor* for cloning into pDONR^{TM}221. Underlined regions are gene-specific, while the remainder of the sequences are Gateway-specific.

Primer Name	Sequence (5'-3')
TvAXEGAT-F	GGGGACAAGTTTGTACAAAAAAGCAGGCTATGTTCTCGTTTAAGGCTGTC
TvAXEGAT-R2	GGGGACCACTTTGTACAAGAAAGCTGGGTCTCATGCGATGCCGAAGAACT
TvAXEGAT-RC	GGGGACCACTTTGTACAAGAAAGCTGGGTCTCCTGCGATGCCGAAGAACT
TvEPGGAT-F	GGGGACAAGTTTGTACAAAAAAGCAGGCTATGTCTGCCTTCGTCCGCCTC
TvEPGGAT-R2	GGGGACCACTTTGTACAAGAAAGCTGGGTCTCACTGCGAGAAGTTCTTGA
TvEPGGAT-RC	GGGGACCACTTTGTACAAGAAAGCTGGGTCTCCCTGCGAGAAGTTCTTGA

Six plasmids were created using pDONR^{TM}221 backbones, with two subtypes (A and B) for each gene to allow for subsequent Gateway cloning (LR reaction) into pEarleyGate plasmids (Earley et al., 2006). The A subtype was specific for cloning into pEarleyGate100 and used the F and R2 primer sets. The B subtype was specific for pEarleyGate101-103 and used the F and RC primer sets. The RC primers remove the native stop codon of the AXE and EPG genes to allow fusion at their C-termini to the fluorescent proteins of pEarleyGate101-103.

3.3. PCR

The polymerase chain reaction mixtures were prepared according to the Platinum^{TM} *Taq* DNA Polymerase High Fidelity (Invitrogen; cat#: 11304011) manual. They were as follows: 13.4 µL of water, 2 µL of 10X PCR buffer, 1 µL $MgSO_4$, 0.5 µL of 10 mM dNTP, 1 µL of forward and reverse primers, 1 µL of cDNA, and 0.1 µL of polymerase for a final volume of 20 µL. The thermocycler conditions were 95°C for 5 min, followed by 35 cycles of 95°C for 30s, 60°C for 30 s, 72°C for 80 s, and finally 72°C for 10 min. The reactions were separated using a 1% agarose gel to isolate the Gateway *att*B-PCR products, which were then excised from the gel.

3.4. Gel Extraction

The PCR products were extracted from agarose gel slices using the PureLink^{TM} Quick Gel Extraction Kit (Invitrogen; cat#: K210012). Briefly, 1.2 mL of gel solubilization buffer (L3) was added to the excised gel and the mixture was incubated at 50°C for 10 min to fully dissolve the agarose gel. The solution was then added to a spin column and centrifuged at 12,000 × g for 1 min, and flow-through was discarded. After adding 500 µL of wash buffer (W1) to the column it was centrifuged at 12,000 × g for 1 min. The

flow-through was removed and then the column was centrifuged for an additional 2 min to remove residual ethanol. Then 50 µL of elution buffer (E5) was added to the spin column before centrifuging at 12,000 × g for 1 min. The resulting DNA was stored at 4°C.

3.5. BP Clonase Reaction

The next step was to insert these PCR products into the pDONR^{TM}221 vector, which is specially designed to integrate *att*B-PCR products. The Gateway® BP Clonase^{TM} II Enzyme Mix (Invitrogen; cat#: 11789-020) was used for this purpose according to the manufacturer's instructions. Briefly, the reaction consisted of the following: 7 µL of *att*B-PCR product, 1 µL of pDONR^{TM}221, and 2 µL of BP clonase II. The solutions were allowed to incubate at 25°C for 18 h. When the reaction was complete, a 1 µL aliquot of Proteinase K was added to the reaction and incubated at 37°C for 10 min.

3.6. LR Clonase Reaction

For Gateway cloning of the AXE and EPG genes into pEarleyGate100-104 from pDONR^{TM}221 constructs, Gateway® LR Clonase^{TM} II Enzyme Mix (Invitrogen; cat#: 11791-020) was used according to the manufacturer's instructions. Briefly, the reaction consisted of the following: 1 µL of pDONR^{TM}221 construct, 1 µL of destination vector (pEarleyGate100-103), 6 µL of TE buffer and 2 µL of LR clonase II. The solutions were allowed to incubate at 25°C for 18 h. When the reaction was complete, a 1 µL aliquot of Proteinase K was added to the reaction and incubated at 37°C for 10 min.

3.7. Transformation of *E.coli*

All transformations were performed with competent One Shot® OmniMAX^{TM} 2 T1 Phage-Resistant Cells (Invitrogen; cat#: C8540-03). An aliquot of 1 µL of the BP or LR

reactions was added to 50 µL of the competent cells. After incubating the cells for 30 min on ice, heat-shocking of the cells was performed by incubating at 42°C for 30 s. Then 250 µL of S.O.C. medium was added to the cells, which were then incubated at 37°C for 1 h with shaking (250 rpm). The cells were then spread onto LB plates containing kanamycin (50 µg/mL) and incubated at 37°C for 16 h.

3.8. Plasmid Isolation

Plasmids were isolated from 4 mL cultures of LB with kanamycin (50 µg/mL) using the PureLink™ Quick Plasmid Miniprep Kit (Invitrogen; cat#: K210010). The cell suspensions (1-4 mL) were centrifuged at 12,000 × g for 3 min to pellet the *E. coli*. For resuspension, 250 µL of resuspension buffer (R3) containing RNase A was added. After resuspension, 250 µL of lysis buffer (L7) was added, followed by inversion mixing and incubation at room temperature for 5 min. Then 350 µL of precipitation buffer (N4) was added, followed by inversion mixing and centrifugation at 12,000 × g for 10 min. After precipitation, the 750 µL of supernatant containing the plasmids was added to a spin column in a 2 mL wash tube and centrifuged at 12,000 × g for 1 min. To wash the samples, 700 µL of wash buffer (W9+ethanol) was added before centrifuging at 12,000 × g for 1 min. The spin column was then centrifuged again at 12,000 × g for 1 min to remove residual ethanol. To elute the plasmids, 35-75 µL of TE buffer was added to the column membrane followed by incubation for 1 min at room temperature and centrifugation at 12,000 × g for 10 min. The samples were stored at 4°C.

3.9. Sequence Analysis

Sanger sequencing was performed at the University of Illinois at Urbana-Champaign (UIUC) Core Sequencing Facility. The samples were provided at a concentration of 100-

200 ng/µL and sequenced using M13 primers for pDONR^{TM}221 constructs, or with gene-specific forward and reverse primers for pEarleyGate constructs (Table 2).

Table 2. Primers used for sequencing *T. versicolor* acetyl xylan esterase (AXE) and endo-polygalacturonase (EPG) from pDONR^{TM}221 (M13 primers) or pEarleyGate constructs (gene-specific primers).

Primer Name	Sequence (5'-3')
M13For-21	GTAAAACGACGGCCAGT
M13Rev-24	AACAGCTATGACCATG
AXE-565F	ACGCTTTGCTCTCGCTAAT
AXE-387R	GAACTTCGAACCCTGGAAGTAG
AXE-718R	CACAGACCTCGTTGAAGGTATC
EPG-266F	GCGGGAAGTCGATCACATTTA
EPG-713F	CCGTCTCTGGCATTGTCATTAG
EPG-387R	CGTTCGTGTAGGTACCAGATATT

3.10. Software

The *T. versicolor* transcriptome data were analyzed using ArrayStar® version 15.2.0 (DNASTAR®, Madison, WI) as previously described (Alanazi, 2018; Alsubaie, 2019). The output from ArrayStar® was exported to Excel for further analysis. The heatmap of the core transcripts was generated using log_2-transformed data and the online expression imaging platform available through heatmapper.ca (Pearson distance method with average clustering functions). Plasmid maps were generated using SeqBuilder Pro^{TM} version 15.2.0 (DNASTAR®).

4. Results and Discussion

4.1. Transcriptome Analysis

To find candidate hemicellulase genes in *T. versicolor* for expression in plant systems, the transcriptome data from previous EIU graduate students who explored *Trametes versicolor* as a pretreatment agent for various forms of biomass was further analyzed (Alanazi, 2018; Alsubaie, 2019). Comparisons between the *T. versicolor* transcriptomes after growth on maple wood, miscanthus straw, and sunflower stems were made with malt extract agar plates serving as the non-biomass control. Using a threshold of 30X or greater expression (for each biomass type compared to the non-biomass control) revealed a core set of 32 transcripts that were highly expressed by the fungus on all three forms of lignocellulose (Figure 1). The core set of transcripts contains several enzymes that act on cellulose, such as cellobiohydrolases (3 transcripts) and endoglucanases (2 transcripts). Notable lignin deconstruction enzymes were also present, such as lignin peroxidases (3 transcripts) and manganese peroxidases (2 transcripts). Two transcripts from the core *T. versicolor* set were identified as hemicellulases: acetyl xylan esterase (AXE; transcript ID: 44147) and endo-polygalacturonase (EPG; transcript ID: 52686). As the name suggests, AXE hydrolyzes the ester bond between acetic acid and xylan (Hettiarachchi et al., 2019), while EPG hydrolyzes the α-1-4 glycosidic bonds within glucuronic acid chains (Federici et al., 2001)(Figure 2).

4.2. Gene Amplification and Entry Clone Creation

Two versions of AXE and EPG were generated through PCR to facilitate two different downstream scenarios. In the first scenario, the entire original open reading frame of both genes (A subtype) were cloned into binary plasmids for expression in plants. In the

second scenario, the native stop codon for AXE and EPG (TGA in both cases) was modified to a glycine codon (GGA) to allow for C-terminal fusion with yellow fluorescent protein (YFP), cyan fluorescent protein (CFP), or green fluorescent protein (GFP).

Both subtypes of each gene were amplified with a high fidelity polymerase and gel purified for cloning into the Gateway entry plasmid pDONR221. This cloning step required the use of the commercial enzyme BP clonase, which uses homologous recombination to replace a DNA cassette containing a chloramphenicol resistance gene (CmR) and the gene for a gyrase toxin (ccdB) (Figure 3). The result is a plasmid without CmR or ccdB genes, which allows viability of transformed *E. coli*. Plasmid maps of pDONR221 containing AXE and EPG (Figure 4a and b) were confirmed by sequencing using the M13 primer sites on either side of the cloning region (Figure 3; Appendix Figures A1 and A2). The *att*L1 and *att*L2 sites of the AXE and EPG entry plasmids (Figure 4a and b) were the result of recombination of the *att*B and *att*P sites found on the PCR products and pDONR221 plasmid, respectively (Figure 5). These attL sites were critical for subsequent cloning into the destination vectors.

4.3. Destination Plasmids

As with the BP clonase reaction described above, the LR clonase reaction of the Gateway system uses homologous recombination to exchange cassettes flanked by the *att*L regions of pDONR-based plasmids with the *att*R regions located on the binary destination plasmids (Figure 6). Destination plasmids contain the *ccdB* and *CmR* genes (described in section 4.2) that prevent *E. coli* from surviving if they receive destination plasmids that did not undergo the homologous recombination event.

The LR clonase reaction was used to transfer the genes for AXE and EPG into pEarleyGate plasmids designed for expression in plants (Earley et al., 2006). Specifically, pEarleyGate100 (Figure 7) was used for the A subtypes, and pEarleyGate101-103 (Figure 8) was used for the B subtypes. The removal of the native stop codon for both genes in the B subtypes allowed for C-terminal fusion with fluorescent proteins (YFP, CFP, and GFP). The result was four pEarleyGate plasmids for each gene (Figures 9 and 10). These plasmids can be sequence confirmed using gene-specific primers to sequence the entire open reading frame of AXE and EPG as well as the fusion areas at the end of the 35S promoter region (for all constructs) and the C-terminal fusion area (for pEarleyGate101-103).

4.4. Binary Plasmid Features

The binary plasmids containing AXE and EPG that were created from pEarleyGate backbones contain several key features for plant transformation. One of the most important features is the 35S promoter that will drive the expression of AXE and EPG in the plant. This well-studied promoter originates from the cauliflower mosaic virus, and allows for constitutive expression of a gene of interest (Benfey and Chua, 1990; Bak and Emerson, 2020). This promoter is particularly useful for the current project because it is unknown what tissues the fungal hemicellulases, AXE and EPG, will affect, if any. If the expression of these microbial enzymes leads to unviable plant transformants or severe phenotypes (e.g. dwarfism), then a more specific and/or less potent promoter may be necessary. For example, the 4CL promoter associated with the generation of lignin in woody plants has been used for the purposes of more directed expression of transgenes (Rogers and Campbell, 2004; Canam et al., 2006).

The binary plasmids in this study also contained the *bar* gene (BLP-R), which was originally discovered in *Streptomyces hygroscopicus* (Thompson et al., 1987). The *bar* gene codes for an enzyme that provides resistance to the herbicide bialaphos (Nakamura et al., 2010). This herbicide is degraded by plants to form phosphinothricin (glufosinate) that prevents normal activity of glutamine synthetase, which causes ammonia to reach unsustainable levels in the plant thereby leading to death (Lutz et al., 2001). Plants that have been successfully transformed with binary vectors containing the *bar* gene are therefore resistant to phosphinothricin, which allows for media-based selection of transgenic plants after the transformation event.

In this study, the binary plasmids created with pEarleyGate101-103 backbones contain fusions of the AXE and EPG genes with the genes for either yellow fluorescent protein (YFP), cyan fluorescent protein (CFP), or green fluorescent protein (GFP). These chimeric genes allow for the C-termini of AXE and EPG to fuse to the N-termini of the fluorescent proteins. These fluorescent proteins contain a chromophore, which is the result of conjugation of amino acids in close proximity to each other (e.g. Ser65, Tyr66, and Gly67 in GFP) in the folded protein structure (Sample et al., 2009). These fusion proteins will be useful in future studies to identify the plant tissues, cell types, and subcellular locations that are expressing the fungal enzymes, using fluorescent microscopy. One of the fluorescent fusion proteins may be adequate for this purpose, although some plant tissues, particularly photosynthetic cells, exhibit auto-fluorescence under wavelengths required for excitation of YPF, CFP, and GFP. The availability of options for fluorescence will allow for greater experimental flexibility in the future.

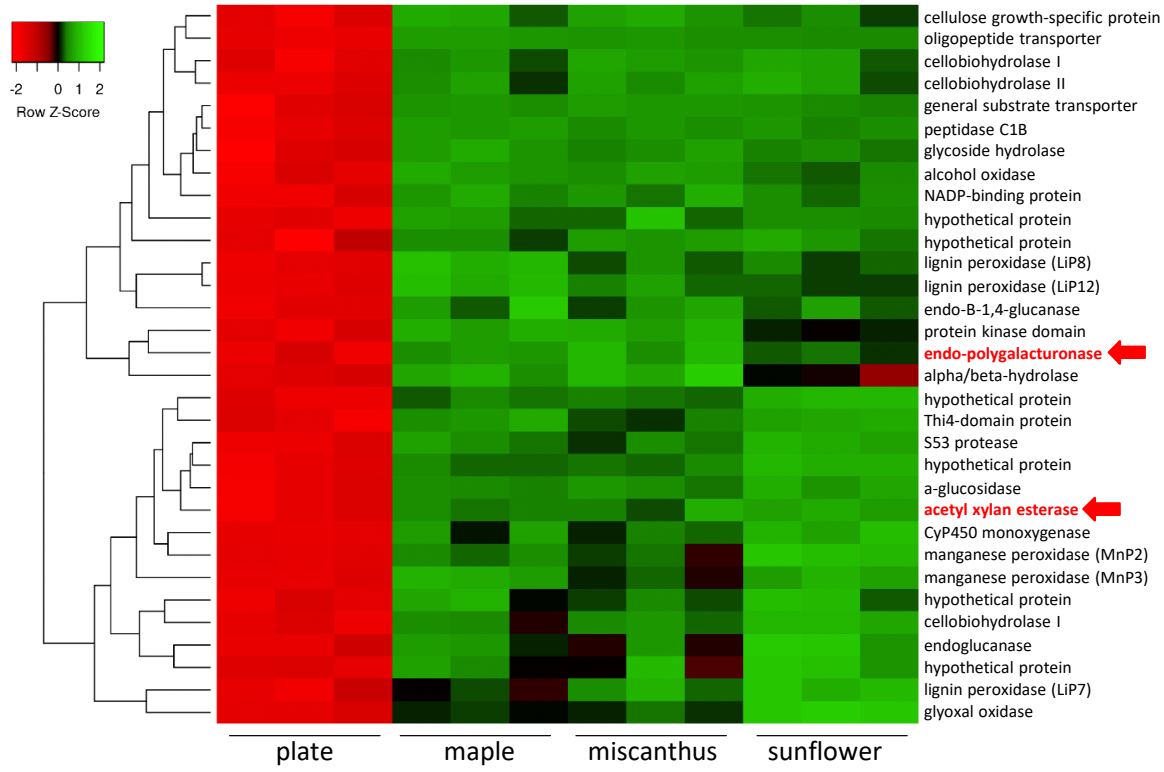

Figure 1. Heatmap of the 32 transcripts from *T. versicolor* with expression of 30X or greater on lignocellulose substrates compared to malt extract agar (plate). The two hemicellulases from this core set of transcripts are indicated by red arrows and font.

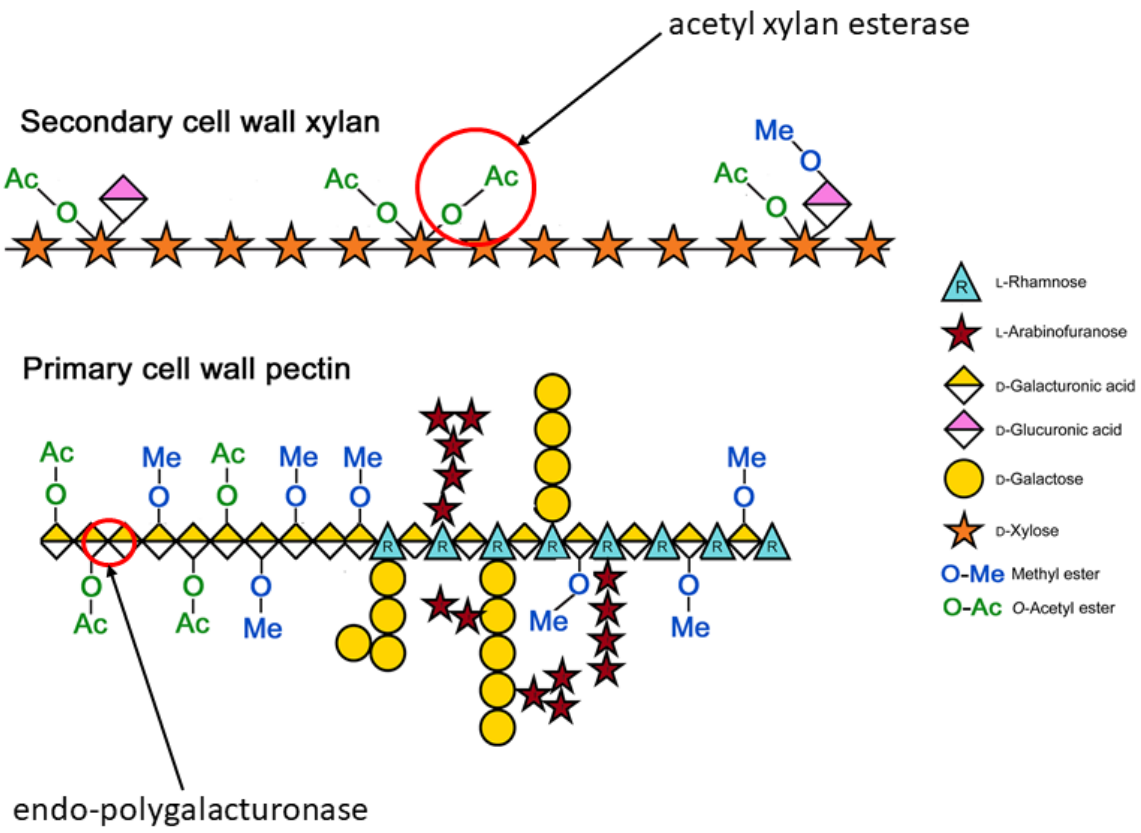

Figure 2. Representation of hemicellulases from the primary and secondary cell walls of plants. Original image from Dewhirst et al. (2020) with circles, arrows, and enzyme names overlaid to emphasize important bonds and reactions.

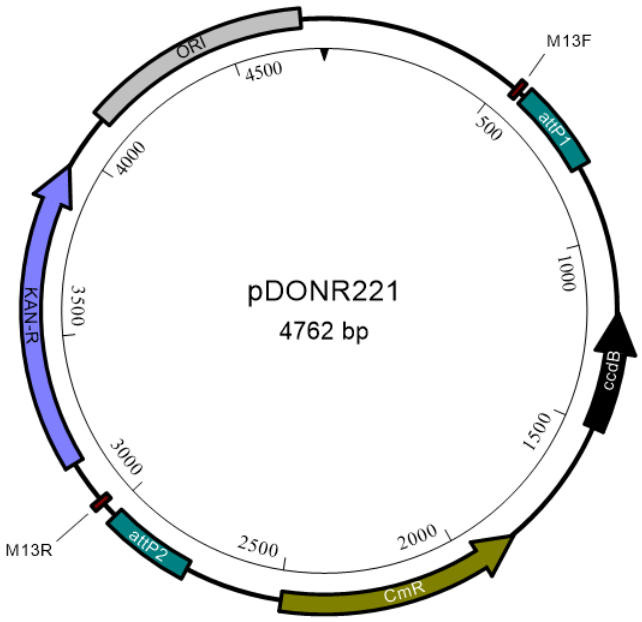

Figure 3. Map of the commercial Gateway entry plasmid pDONR221. M13F: M13 forward primer binding site, *att*P1: Gateway-specific cloning sequence, ccdB: gyrase toxin gene, CmR: chloramphenicol resistance gene, *att*P2: Gateway-specific cloning sequence, M13R: M13 reverse primer binding site, KAN-R: kanamycin resistance gene, ORI: origin of replication.

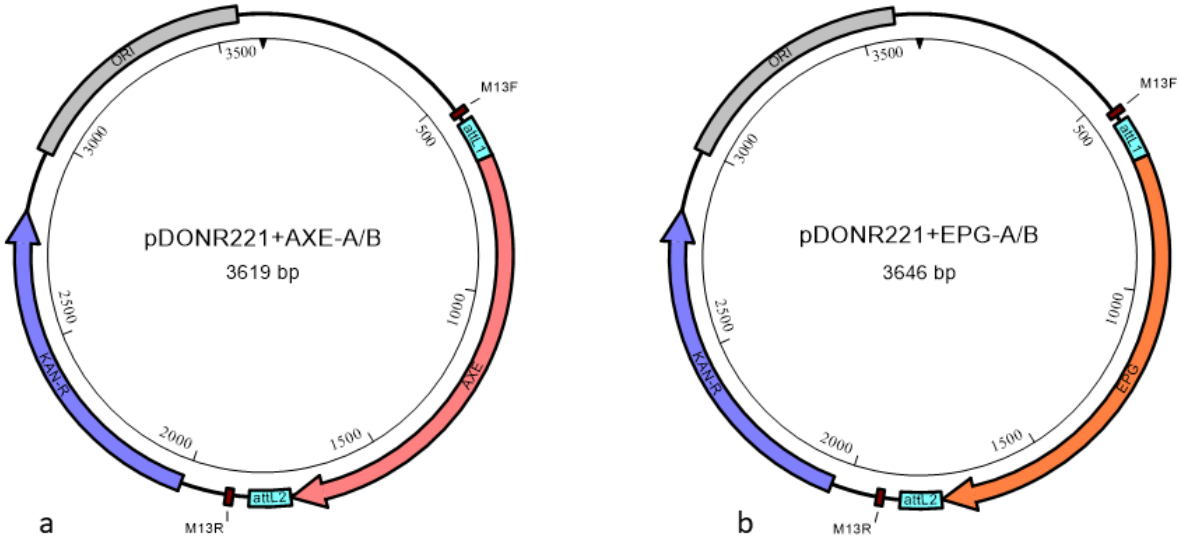

Figure 4. Maps of the pDONR221 constructs containing AXE (a) and EPG (b). Both the A and B subtypes of each gene are represented with one map because of the identical sequence lengths (only the sequence of the stop codon has changed). Features are as described in Figure 3.

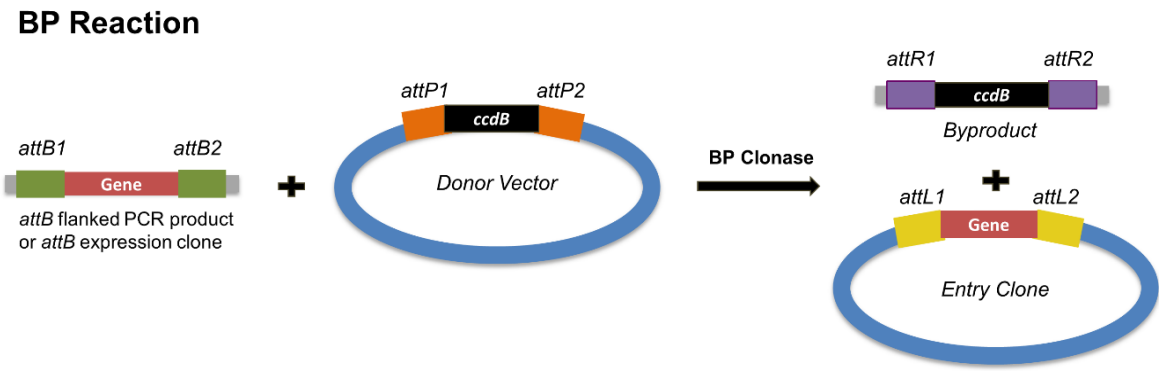

Figure 5. The BP clonase reaction illustrating the homologous recombination event between an *att*B-flanked PCR products and entry plasmid containing *att*P sequences (image courtesy of addgene.org).

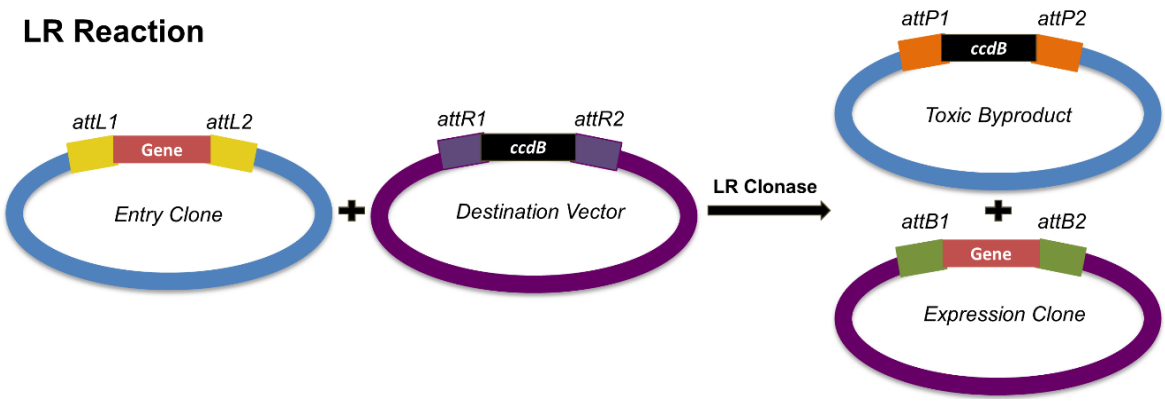

Figure 6. The LR clonase reaction illustrating the homologous recombination event between an entry plasmid containing *att*L sequences and a destination plasmid containing *att*R sequences (image courtesy of addgene.org).

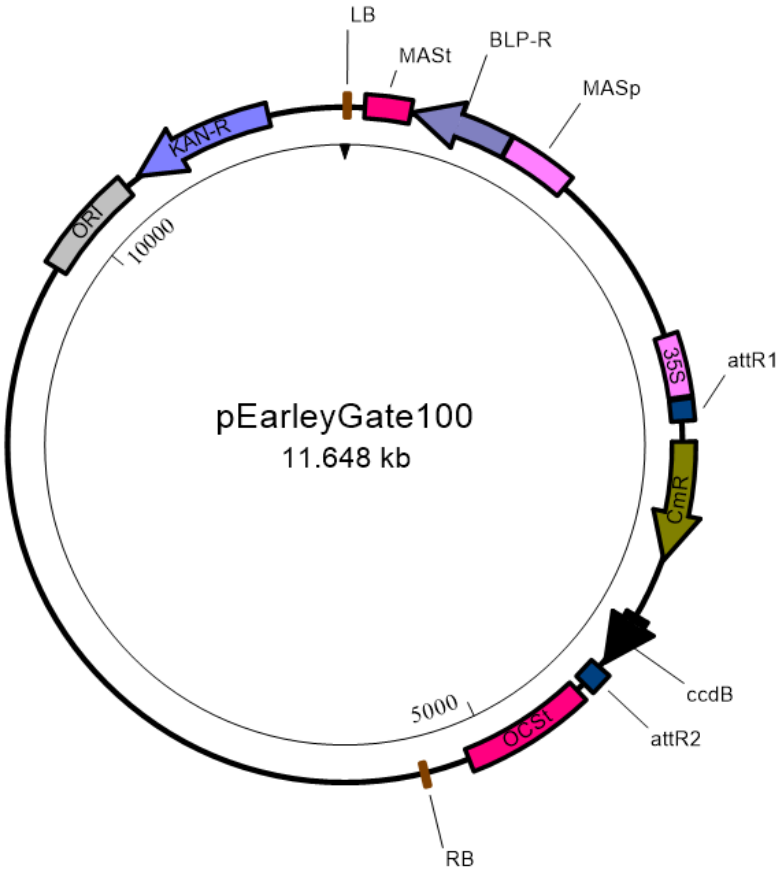

Figure 7. Map of the pEarleyGate100 binary plasmid for plant transformation. ORI: origin of replication, KAN-R: kanamycin resistance gene, LB: left border of binary plasmid, MASt: mannopine synthase terminator, BLP-R: bialaphos resistance gene, MASp: mannopine synthase promoter, 35S: cauliflower mosaic virus 35S promoter, *att*R1: Gateway-specific cloning sequence, CmR: chloramphenicol resistance gene, *ccdB*: gyrase toxin gene, *att*R2: Gateway-specific cloning sequence, OCSt: octopine synthase terminator, RB: right border of binary plasmid.

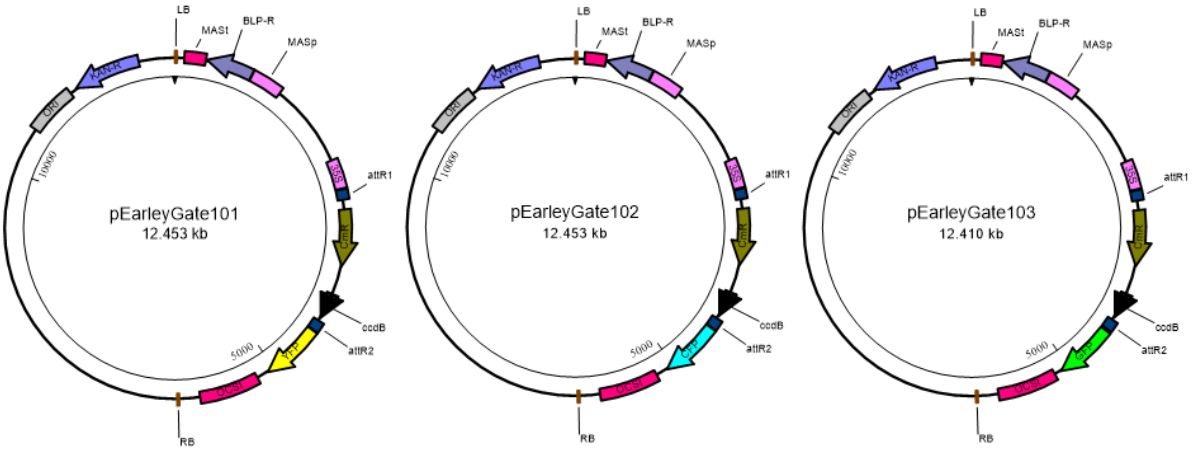

Figure 8. Maps of pEarleyGate101-103. The difference between the three plasmids is the fluorescent protein gene (YFP, CFP, or GFP). Features are as described in Figure 7.

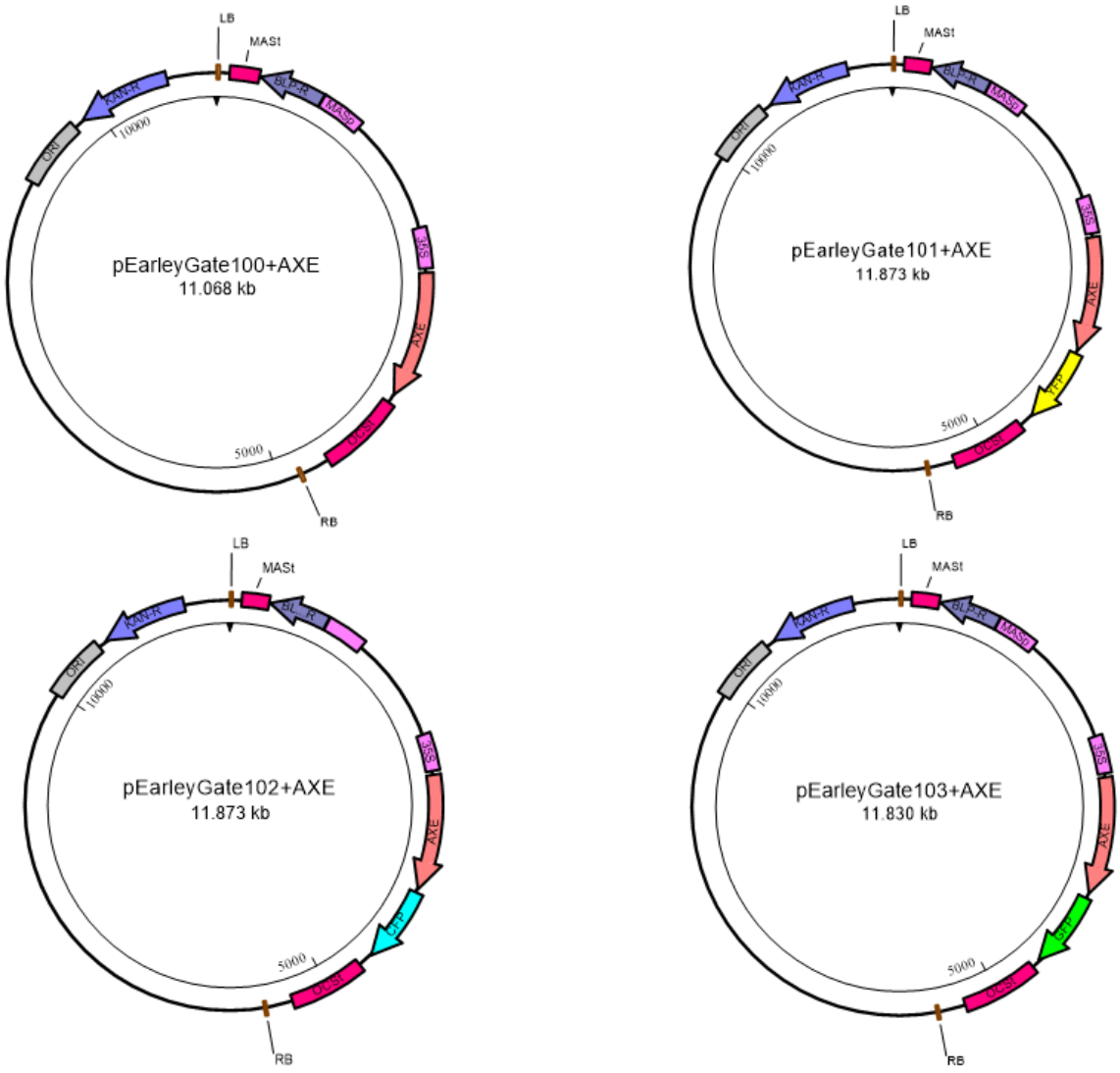

Figure 9. The pEarleyGate-based constructs containing the acetyl xylan esterase (AXE) gene. pEarleyGate100+AXE has the A subtype gene with the native stop codon, while pEarleyGate101-103 constructs have the B subtype with the stop codon converted to GGA to allow fusion to the fluorescent proteins. Features are as described in Figure 7.

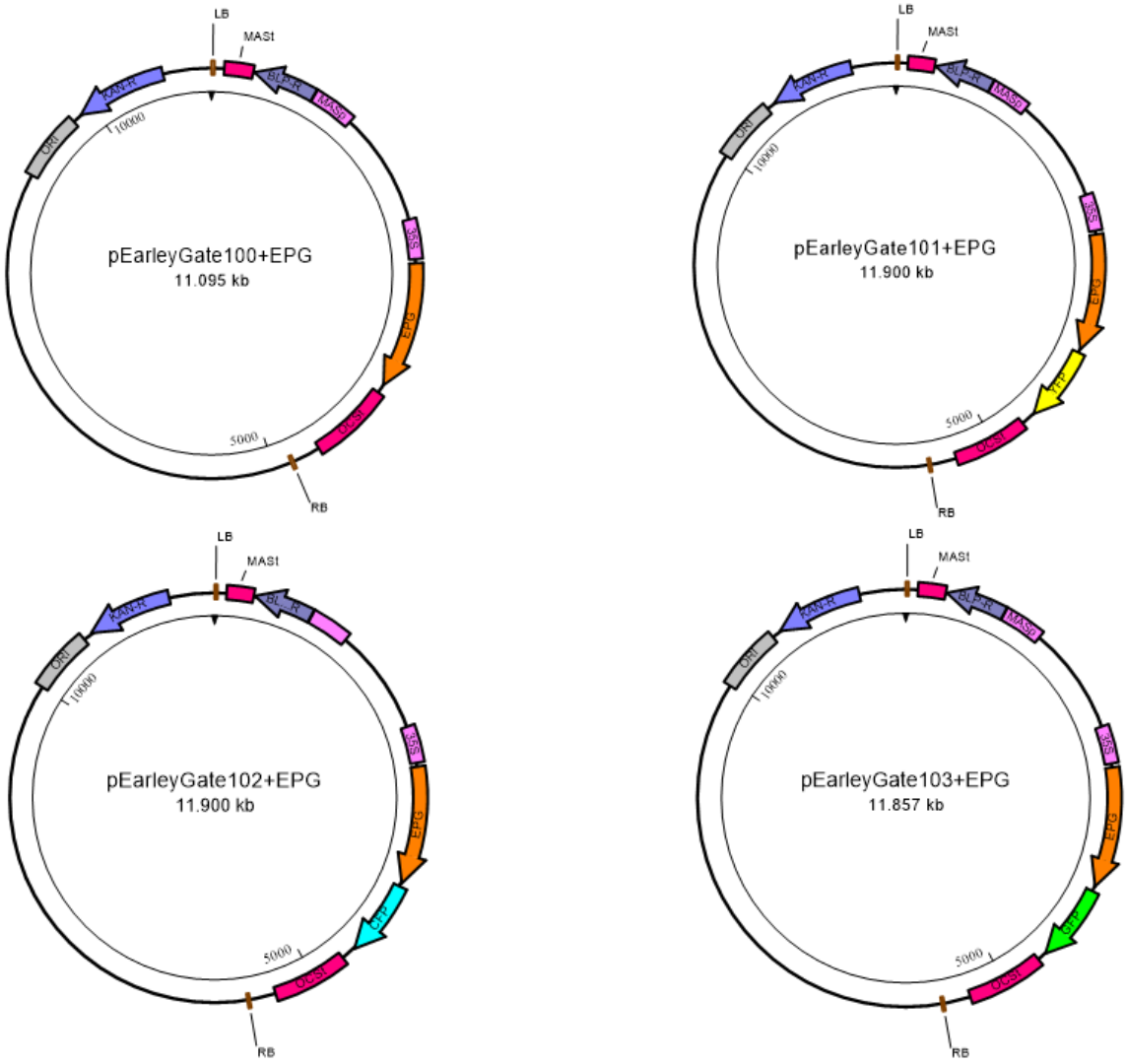

Figure 10. The pEarleyGate-based constructs containing the endo-polygalacturonase (EPG) gene. pEarleyGate100+EPG has the A subtype gene with the native stop codon, while pEarleyGate101-103 constructs have the B subtype with the stop codon converted to GGA to allow fusion to the fluorescent proteins. Features are as described in Figure 7.

5. Conclusions

This research project generated eight binary plasmids containing acetyl xylan esterase (AXE) and endo-polygalacturonase (EPG), which were shown to be highly expressed by the white-rot fungus, *Trametes versicolor*, when grown on a variety of lignocellulosic substrates. These plasmid constructs will facilitate the constitutive expression of AXE and EPG in model plant systems, such as *Arabidopsis thaliana*, *Nicotiana tabacum*, and *Populus tremula* x *alba*. The constructs provide the choice of expressing the genes in their native form (with pEarleyGate100 backbones) or as fusions with fluorescent proteins (with pEarleyGate101-103 backbones). The fungal AXE and EPG enzymes have the potential to alter the cell wall chemistry of transformed plants, particularly with respect to hemicellulosic linkages among lignocellulose. It is anticipated that these changes could lead to changes in lignin extractability and glucose yield by mitigating the recalcitrance of plant cells walls, which is a formidable obstacle for the generation of liquid fuels from lignocellulosic biomass.

6. References

Alanazi, Maha, "The Transcriptional Response of *Trametes versicolor* to Growth on Maple Chips and Miscanthus Straw" (2018). *Masters Theses*. 4579. https://thekeep.eiu.edu/theses/4579.

Alaradi, Mashael Rashed, "The Transcriptome Response of the White-Rot Fungus *Phanerochaete chrysosporium* to Maple and Miscanthus" (2017). *Masters Theses*. 4292. https://thekeep.eiu.edu/theses/4292.

Alsubaie, Nadh Hamoud, "The Transcriptional Response of *Phanerochaete Chrysosporium* and *Trametes Versicolor* to Growth on Stems of *Helianthus Argophyllus* (Silverleaf Sunflower)" (2019). *Masters Theses*. 4474. https://thekeep.eiu.edu/theses/4474

Bak, A., & Emerson, J. B. (2020). Cauliflower mosaic virus (CaMV) biology, management, and relevance to GM plant detection for sustainable organic agriculture. *Frontiers in Sustainable Food Systems*, 4, 21.

Benfey, P. N., & Chua, N. H. (1990). The cauliflower mosaic virus 35S promoter: combinatorial regulation of transcription in plants. *Science*, 250(4983), 959-966.

Canam, T., Park, J.Y., Yu, K.Y. et al. (2006) Varied growth, biomass and cellulose content in tobacco expressing yeast-derived invertases. *Planta* 224, 1315–1327.

Canam, T., Town, J. R., Tsang, A., McAllister, T. A. & Dumonceaux, T. J. (2011). Biological pretreatment with a cellobiose dehydrogenase-deficient strain of *Trametes versicolor* enhances the biofuel potential of canola straw. *Bioresource Technology*, 102, 10020–10027.

Canam, T., Town, T., lroba, K., Tabil, L., & Dumonceaux, T.J. (2013a) "Pretreatment of lignocellulosic biomass using microorganisms: Approaches, advantages, and limitations" in Sustainable Degradation of Lignocellulose Biomass - Techniques, Applications and Commercialization. Eds. Chandel, A.K. and da Silva, S.S. InTech publishing.

Canam, T., Dumonceaux, T.J., Record, E., & Li, Y.B. (2013b) White Rot Fungi: The key to sustainable biofuel production? *Biofuels*. 4, 247-250.

Ciriminna, R., Albanese, L., Pecoraino, M., Meneguzzo, F., & Pagliaro, M. (2019). Solar energy and new energy technologies for mediterranean countries. *Global Challenges*, 3(10), 1900016.

Dewhirst, R. A., Afseth, C. A., Castanha, C., Mortimer, J. C., & Jardine, K. J. (2020). Cell wall O-acetyl and methyl esterification patterns of leaves reflected in atmospheric emission signatures of acetic acid and methanol. *PLoS ONE*, 15(5), e0227591.

Earley, K. W., Haag, J. R., Pontes, O., Opper, K., Juehne, T., Song, K., & Pikaard, C. S. (2006). Gateway-compatible vectors for plant functional genomics and proteomics. *The Plant Journal*, 45(4), 616-629.

Federici, L., Caprari, C., Mattei, B., et al. (2001). Structural requirements of endopolygalacturonase for the interaction with PGIP (polygalacturonase-inhibiting protein). *Proceedings of the National Academy of Sciences*, 98(23), 13425-13430.

Floudas, D., Binder, M., Riley, R., et al. (2012). The Paleozoic origin of enzymatic lignin decomposition reconstructed from 31 fungal genomes. *Science*, 336, 1715–1719.

Hettiarachchi, S. A., Kwon, Y. K., Lee, Y., et al. (2019). Characterization of an acetyl xylan esterase from the marine bacterium *Ochrovirga pacifica* and its synergism with xylanase on beechwood xylan. *Microbial Cell Factories*, 18(1), 122.

Kalinoski, R. M., Flores, H. D., Thapa, S., Tuegel, E. R., Bilek, M. A., Reyes-Mendez, E. Y., West, M. J., Dumonceaux, T. J. & Canam, T. (2017). Pretreatment of hardwood and miscanthus with *Trametes versicolor* for bioenergy conversion and densification strategies. *Applied Biochemistry & Biotechnology*, 183, 1401-1413.

Kumar, P., Barrett, D. M., Delwiche, M. J. & Stroeve, P. (2009). Methods for pretreatment of lignocellulosic biomass for efficient hydrolysis and biofuel production. *Industrial & Engineering Chemistry Research*, 48, 3713–3729.

Latha Gandla, M., Derba-Maceluch, M., Liu, X., Gerber, L., Master, E. R., Mellerowicz, E. J., & Jönsson, L. J. (2015). Expression of a fungal glucuronoyl esterase in *Populus*: effects on wood properties and saccharification efficiency. *Phytochemistry*, 112, 210–220.

Lin, L., Xu, F., Ge, X., & Li, Y. (2016). Improving the sustainability of organic waste management practices in the food-energy-water nexus: A comparative review of anaerobic digestion and composting. *Renewable and Sustainable Energy Reviews*, 89, 151-167.

Lutz, K. A., Knapp, J. E., & Maliga, P. (2001). Expression of bar in the plastid genome confers herbicide resistance. *Plant Physiology*, 125(4), 1585-1590.

MacDonald, J., Doering, M., Canam, T., Gong, Y., Guttman, D. S., Campbell, M. M. & Master, E. R. (2011). Transcriptomic responses of the softwood-degrading white-rot fungus *Phanerochaete carnosa* during growth on coniferous and deciduous wood. *Applied and Environmental Microbiology*, 77, 3211–3218.

MacDonald, J. & Master, E. R. (2012). Time-dependent profiles of transcripts encoding lignocellulose-modifying enzymes of the white rot fungus *Phanerochaete carnosa* grown on multiple wood substrates. *Applied and Environmental Microbiology*, 78, 1596–1600.

McKendry, P. (2002). Energy production from biomass (part 1): overview of biomass. *Bioresource Technology*, 83(1), 37-46.

Nakamura, S., Mano, S., Tanaka, Y., et al. (2010). Gateway binary vectors with the bialaphos resistance gene, *bar*, as a selection marker for plant transformation. *Bioscience, Biotechnology, and Biochemistry*, 74(6), 1315-1319.

Okamoto, K., Nitta, Y., Maekawa, N., & Yanase, H. (2011). Direct ethanol production from starch, wheat bran and rice straw by the white rot fungus *Trametes hirsuta*. *Enzyme and Microbial Technology*, 48(3), 273-277.

Renewable Fuels Association. (2017). 2017 Ethanol Industry Outlook. http://www.ethanolrfa.org/wp-content/uploads/2017/02/Ethanol-Industry-Outlook-2017.pdf.

Rogers, L. A., & Campbell, M. M. (2004). The genetic control of lignin deposition during plant growth and development. *New Phytologist*, 164(1), 17-30.

Sample, V., Newman, R. H., & Zhang, J. (2009). The structure and function of fluorescent proteins. *Chemical Society Reviews*, 38(10), 2852-2864.

Sánchez, C. (2009). Lignocellulosic residues: biodegradation and bioconversion by fungi. *Biotechnology Advances*, 27(2), 185-194.

Sanchez, O. J., & Cardona, C. A. (2008). Trends in biotechnological production of fuel ethanol from different feedstocks. *Bioresource Technology*, 99(13), 5270-5295.

Shafiei, S., & Salim, R. A. (2014). Non-renewable and renewable energy consumption and CO_2 emissions in OECD countries: a comparative analysis. *Energy Policy*, 66, 547-556.

Suzuki, H., MacDonald, J., Syed, K., et al. (2012). Comparative genomics of the white-rot fungi, *Phanerochaete carnosa* and *P. chrysosporium*, to elucidate the genetic basis of the distinct wood types they colonize. *BMC Genomics*, 13, 444.

Thompson, C. J., Movva, N. R., Tizard, R., Crameri, R., Davies, J. E., Lauwereys, M., & Botterman, J. (1987). Characterization of the herbicide-resistance gene *bar* from *Streptomyces hygroscopicus*. *The EMBO Journal*, 6(9), 2519-2523.

Troisi, G., Barton, S., & Bexton, S. (2016). Impacts of oil spills on seabirds: Unsustainable impacts of non-renewable energy. *International Journal of Hydrogen Energy*, 41(37), 16549-16555.

Tsai, A. Y., Canam, T., Gorzsás, A., Mellerowicz, E. J., Campbell, M. M., & Master, E. R. (2012). Constitutive expression of a fungal glucuronoyl esterase in Arabidopsis reveals altered cell wall composition and structure. *Plant Biotechnology Journal*, 10(9), 1077–1087.

Van Acker, R., Leplé, J. C., Aerts, D., et al. (2014). Improved saccharification and ethanol yield from field-grown transgenic poplar deficient in cinnamoyl-CoA reductase. *Proceedings of the National Academy of Sciences*, 111(2), 845-850.

Wang, Z., Pawar, P. M., Derba-Maceluch, M., Hedenström, M., Chong, S. L., Tenkanen, M., Jönsson, L. J., & Mellerowicz, E. J. (2020). Hybrid aspen expressing a carbohydrate esterase family 5 acetyl xylan esterase under control of a wood-specific promoter shows improved saccharification. *Frontiers in Plant Science*, 11, 380.

Zhao, X., Zhang, L., & Liu, D. (2012). Biomass recalcitrance. Part I: the chemical compositions and physical structures affecting the enzymatic hydrolysis of lignocellulose. *Biofuels, Bioproducts, & Biorefining*, 6, 465-482.

7. Appendix

ATGTTCTCGTTTAAGGCTGTCCTAGGTCTTTGTGCTCTTCTCCCGTCAGTCCTCGCACAGGCGGCAGTGTTCGGGCAGT

GTGGAGGCCAAGGCTTCACAGGCCCCACGACATGCGCATCCGGCTCTACTTGTGTTGAACAGAATGCTTTCTTCTCCCA

GTGCCTGCCCAGCGCGTCCGCTCCGCCCACGACCACGGTCGCTGCGCCCCCTCCCAGCGGCGCCGCGCCGACAGATCTC

AGCGCTATTCCGGCGTCGACGCTGCACCAGATCACCAACTTCGGCACGAACCCCAATAATGTGGGCATGTTCGTGTACA

AGCCCAAGAAGCTGCAGGCGAAGCCGCCCCTGATCGTCGCAAGCCACTTCTGCACAGGTACTGCACAGATCTACTTCCA

GGGTTCGAAGTTCGCGCAACTCGCCGAGACTTTCGGTTACTTGGTCATCTTCCCCTCATCGCCTCATCCCGACTTGTGC

TGGGACGTCTCCTCTGCTCAGACTCTTATGCACAATGGCGGCAGCGATTCGCTCAGTATCGCTAACGTCGCACGCTTTG

CTCTCGCTAATTGGGGCGTCGACCCGAACCGTGTCTTCGCCGTCGGCACGTCCTCGGGCGCGATGATGACCAGCGTGCT

CGCCGGTGCGTACCCGGATATCTTCAAGGCTGGAATCGTGGACTCCGGCGTCGCCTTCGGTTGCTTCGCTTCATCAGGG

CCTCTGGATACCTTCAACGAGGTCTGTGCGTCTGGAAACGTCATCATGACGGGCCAGCAATGGGCTCAGAAGGTCTTCA

ACGCATTCCCGGGCTTCACCGGTACTCGCCCGAAGATCCAGACCTGGCATGGAACAGCCGACACCACCGTGTTCCCACA

GAACTTCTTCGAACAAATCAAACAATGGACGACCGTGTTTGGCCTGCCGAGCACGCCCGTGTCGAACGTCAGCGAGTCG

TTCCTTCCGAAGGGCTACTCGAACGCCACGTTTGGCCCGCAGTTCCAGGCTATCCTCGCACAGGGCGTCGGCCACACCG

TTCCGCTCTTCGAGCAGCAGTACCTCCAGTTCTTCGGCATCGCATGA

MFSFKAVLGLCALLPSVLAQAAVFGQCGGQGFTGPTTCASGSTCVEQNAFFSQCLPSASAPPTTTVAAPPPSGAAPTDL

SAIPASTLHQITNFGTNPNNVGMFVYKPKKLQAKPPLIVASHFCTGTAQIYFQGSKFAQLAETFGYLVIFPSSPHPDLC

WDVSSAQTLMHNGGSDSLSIANVARFALANWGVDPNRVFAVGTSSGAMMTSVLAGAYPDIFKAGIVDSGVAFGCFASSG

PLDTFNEVCASGNVIMTGQQWAQKVFNAFPGFTGTRPKIQTWHGTADTTVFPQNFFEQIKQWTTVFGLPSTPVSNVSES

FLPKGYSNATFGPQFQAILAQGVGHTVPLFEQQYLQFFGIA

Figure A1. Nucleotide (top) and predicted amino acid (bottom) sequences of the acetyl xylan esterase gene cloned from *T. versicolor*. Sequencing of DNA performed using M13 forward and reverse primers from the pDONR221 construct.

ATGTCTGCCTTCGTCCGCCTCGCCGCCCTCCTCGTCTTCGCGCGCGTCACGCTCGCCGCGCCGTCGGCGACCGACTGCA

CGGGCACGATCTCGTCGTTGGACGACGTCGCCGCCGCGGTCAAGTGCACGACCGTGAACATCAACTCGTTCACCGTGCC

CGCCGGGGAGACGTTCAACCTCGACCTCGCGACGGGCACGACCGTGAACATGCAGGGCGACGTGACCTTCGCCGTCAAG

AACTGGGACGGCCCTCTCTTCCAAGTCGGCGGGAAGTCGACCACATTTAACGGTAACGGACATACGTTCGATGGGAACG

GCCCATCGTACTGGGATGGCCAGGGTGGCAATGGCGGTGTCACCAAGCCGGCGCCCATGATGAAGATCAAAATATCTGG

TACCTACACGAATGTGAAGGTTCTTAACTCGCCGGCCCGGGTCTACAGTGTCTCGAACCCCGCAGCGCTCACCATGTCG

AAGCTGACCATCGACGACTCTGCCGGAGATGCCCCCAACTCGAAGAGCGACGGCAAGGCTGCCGGCCACAACACCGACG

GATTTGACGTCAGCACGACTGACTTGACCATCGAGGACAGCACCATTCACAACCAGGATGACTGCCTGGCCATCAACAA

GGGCAGCAACATCGTCTTCCAGCGCAACACCTGCACAGGCGGCCACGGTATCTCGGTCGGCTCTATCGACTCCGACGTC

ACCGTGTCCGGGATTGTCATCAGCGGCAACACCATCACGAACAACGACCAAGCGCTGCGCATCAAGACCAAGTCCGCCG

CATCGTCCTCGACCGTCACGAACACCACCTACTCCGGGAACACCGGAACCGGCCTCCGCCAGTTCGGTGTCCTCATTGA

CCAGAGCTACCCCGACACCCTCGGCACGCCCGGAACCGGCGTCAAGCTGTCCGGCGTGAACTTCGTCGGCGCGACCAAC

AGCCTCACCGTGAACAGCGACGCCGAGCGCGTCGCCGTCAACTGCGGCTCCGGCTCCTGCACCGGTACCTGGGACTGGT

CTGCGCTGAAGGTGACGGGCGGCAAGGCGGGCCCGATCACGAACTTCTCCGGGATCAAGAACTTCTCGCAGTGA

MSAFVRLAALLVFARVTLAAPSATDCTGTISSLDDVAAAVKCTTVNINSFTVPAGETFNLDLATGTTVNMQGDVTFAVK

NWDGPLFQVGGKSTTFNGNGHTFDGNGPSYWDGQGGNGGVTKPAPMMKIKISGTYTNVKVLNSPARVYSVSNPAALTMS

KLTIDDSAGDAPNSKSDGKAAGHNTDGFDVSTTDLTIEDSTIHNQDDCLAINKGSNIVFQRNTCTGGHGISVGSIDSDV

TVSGIVISGNTITNNDQALRIKTKSAASSSTVTNTTYSGNTGTGLRQFGVLIDQSYPDTLGTPGTGVKLSGVNFVGATN

SLTVNSDAERVAVNCGSGSCTGTWDWSALKVTGGKAGPITNFSGIKNFSQ

Figure A2. Nucleotide (top) and predicted amino acid (bottom) sequences of the endo-polygalacturonase gene cloned from *T. versicolor*. Sequencing performed using M13 forward and reverse primers from the pDONR221 construct.